Supporting Information

In-situ-engineered coral-like multiphase NC@NiCoCu-N/NCF nanoarrays for enhanced hydrogen evolution reaction

Yaoxia Yang*,§, Lan Zhang§, Fengyao Guo, Dangxia Wang, Xingwei Guo,

Wei Zeng, and Dongfei Sun

Key Laboratory of Eco-functional Polymer Materials of the Ministry of Education,

Key Laboratory of Eco-environmental Polymer Materials of Gansu Province,

College of Chemistry and Chemical Engineering, Northwest Normal University,

Lanzhou 730070, China

*Corresponding author.

E-mail address: yangyaoxia2007@126.com; yaoxiayang@nwnu.edu.cn (Y-X, Yang).

Experimental Section

Sample Characterization

The physico-chemical structures of the catalysts are investigated with following instruments. The components and morphologies of samples were characterized by using transmission electron microscopy (TEM, FEI TECNAI G^2 F_{20}, America) and field-emission scanning electron microscopy (FE-SEM, Carl Zeiss Ultra Plus, Germany). The elemental mappings and chemical compositions of the samples were characterized via energy-dispersive X-ray spectroscopy (EDX, Oxford, England) equipped with an Aztec-X-80. The crystalline phases and chemical states of resulting were analyzed with an X-ray powder diffraction (XRD, Rigaku D/Max-2400) using a Cu Kα radiation source and X-ray photoelectron spectrometer (XPS, Thermo ESCALAB 250XI) equipped a Al Kα radiation source. Raman spectroscopy (Renishaw invia, England) was used to characterize the structure of carbon materials in the samples.

Electrochemical measurements

All electrochemical measurements are made using Autolab PGSTAT128N (Switzerland) Electrochemical workstation. In a standard three-electrode system, the prepared sample was used as the self-supported working electrode, the graphite electrode as the counter electrode, and the Ag/AgCl and Hg/HgO electrodes as the reference electrodes in 0.5 M H_2SO_4 and 1M KOH solutions, respectively. Linear sweep voltammetry (LSV) curve scanning speed is 5 mV s^{-1}, and all datas are not compensated by iR. The Tafel plot of the linear region is obtained by fitting the Tafel

equation ($\eta = a + b \log j$), where η is overpotential, b is Tafel slope, and j is current density. Since ECSA = C_{dl}/C_s, Electrochemically active surface area (ECSA) is linearly dependent on double-layer capacitance (C_{dl}), ECSA could be assessed by C_{dl} that was obtained from CV cycle curves at 20-100 mV s^{-1} sweep velocities in 1 M KOH and 80-240 mV s^{-1} sweep velocities in 0.5 M H_2SO_4 at nonfaradaic potential range without polarization current. By plotting the current density variation ($\Delta j = (j_a - j_c)/2$) at -0.80 V (vs. RHE) in 1 M KOH and 0.05 V (vs. RHE) in 0.5 M H_2SO_4 with scan rates from CV curves, a slope of the fitting line was observed as Cdl, Electrochemical impedance spectroscopy (EIS) measurements were recorded in the frequency range of 0.01 Hz to 100 kHz with an applied potential of η_{10} and a voltage amplitude of 5 mV. The stability of the catalyst was evaluated by using chronopotentiometric method for 48 h under current densities of 10 mA·cm^{-2} and 50 mA·cm^{-2}.

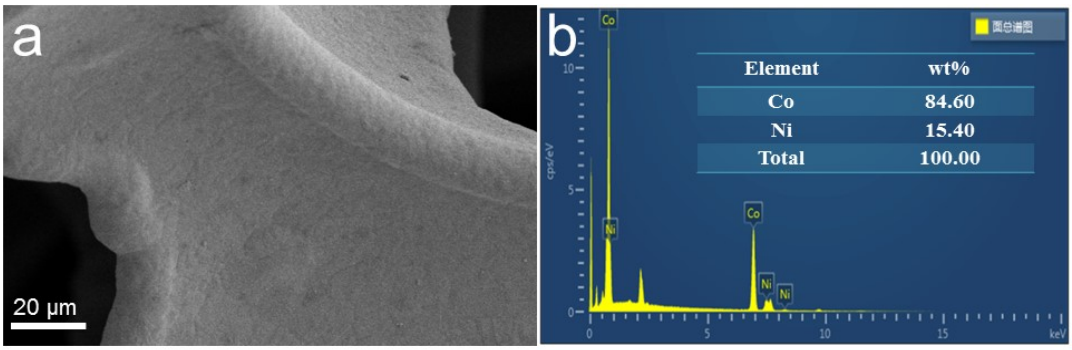

Fig. S1 (a) SEM image of NCF, (b) The EDX spectrum of NCF and corresponding element ratios.

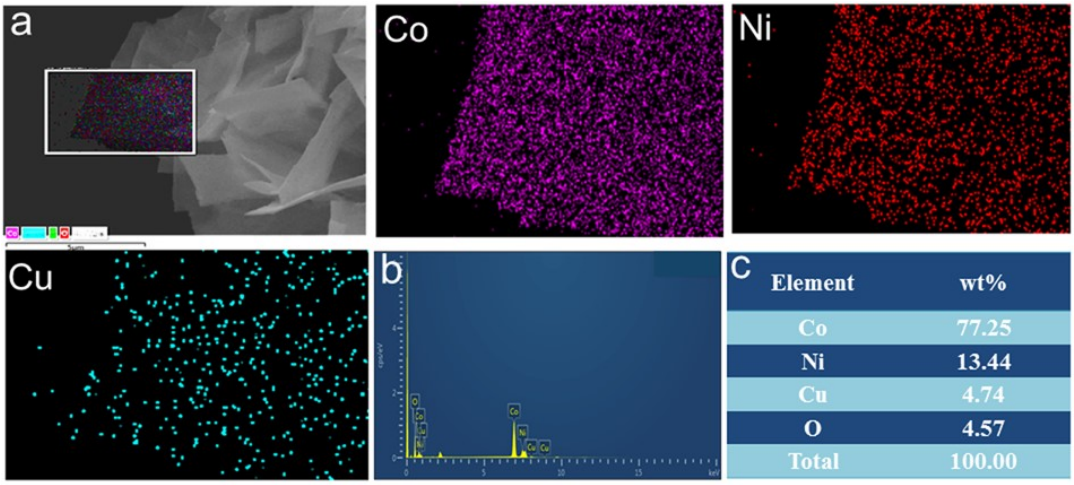

Fig. S2 (a) SEM image and EDX elemental mapping of Co, Ni, Cu and N for Cu/NCF sample, (b) the EDX spectrum of Cu/NCF and corresponding element ratios.

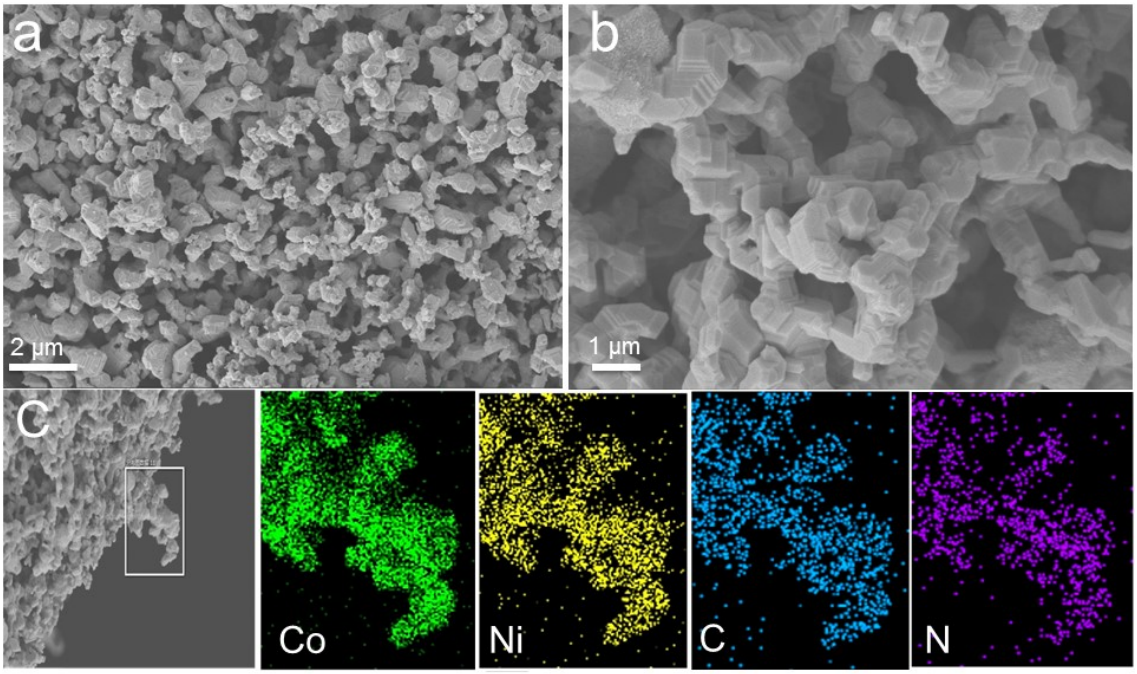

Fig. S3 (a, b) different-resolution SEM images of NiCo-N/NCF, (c) SEM image and EDX elemental mapping of Co, Ni, C and N for NiCo-N/NCF.

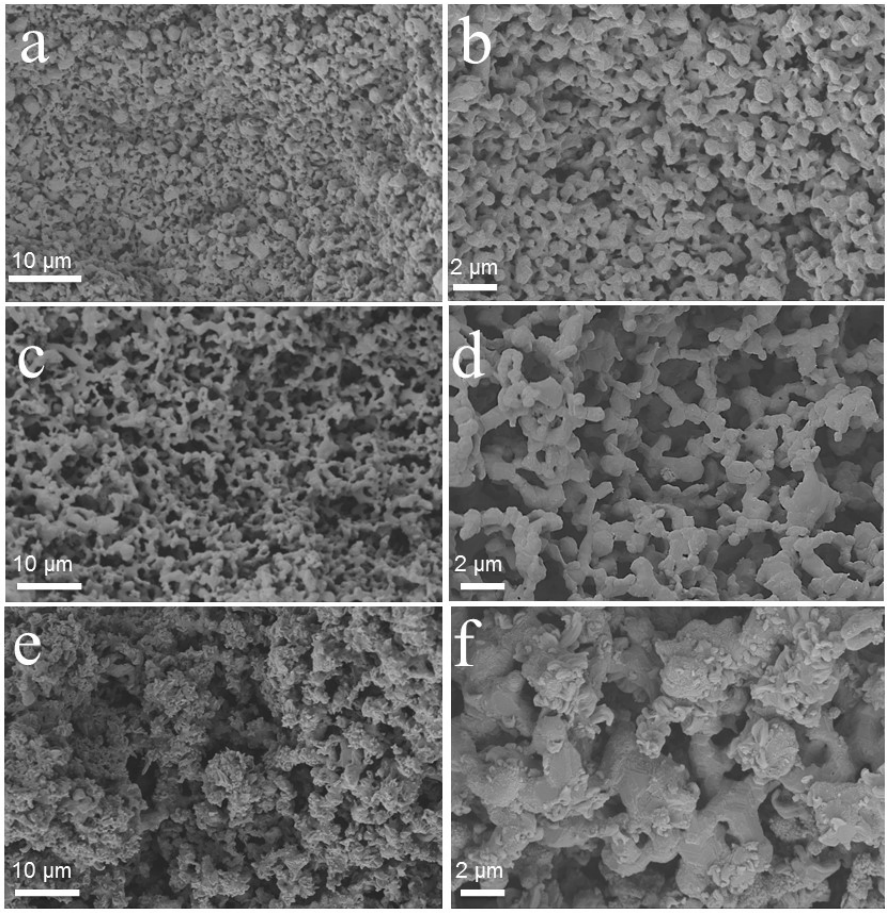

Fig. S4 different-resolution SEM images of samples prepared with (a, b) 0.4 g, (c, d) 0.5 g and (e, f) 0.6 g dicyandiamide in the nitriding process.

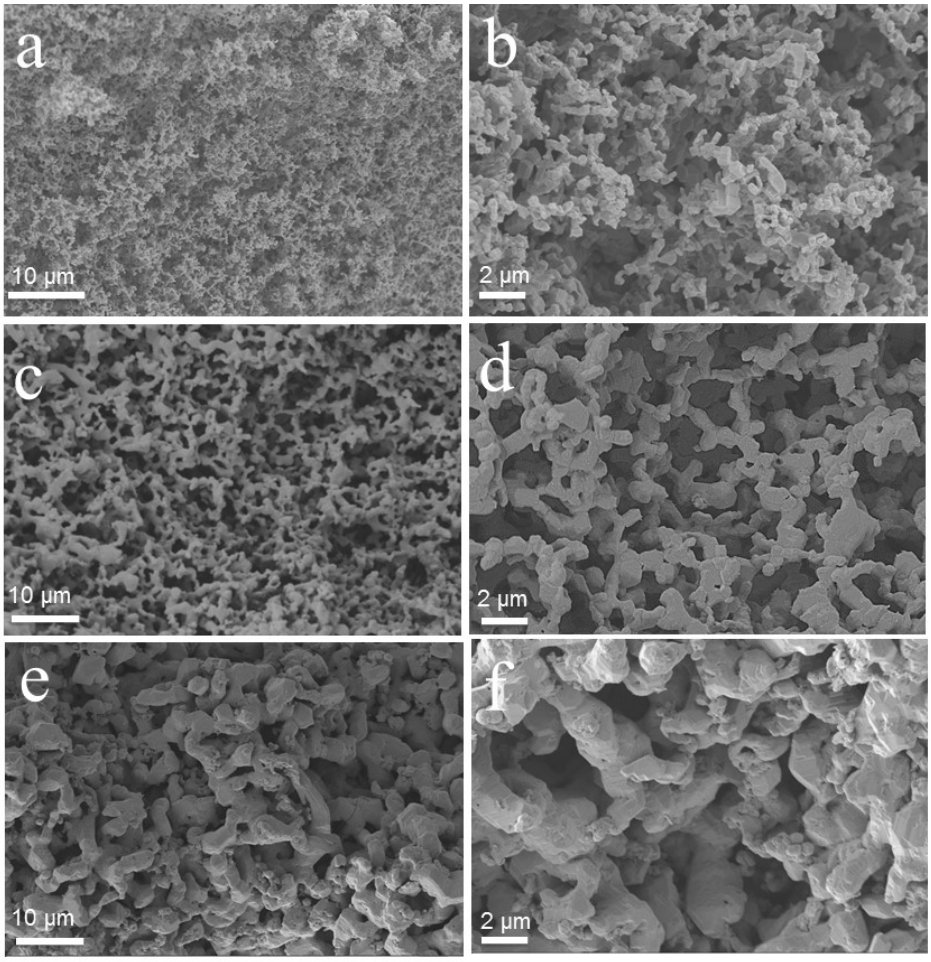

Fig. S5 different-resolution SEM images of samples prepared with (a, b) 600 ºC, (c, d) 700 ºC and (e, f) 800 ºC temperature in the nitriding process.

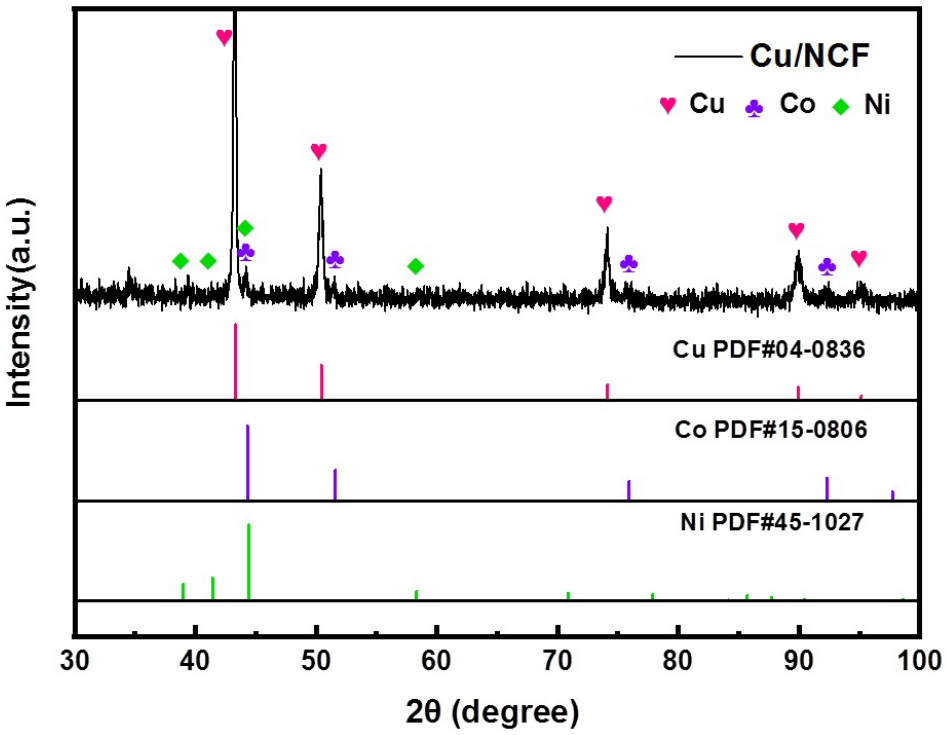

Fig. S6 The XRD patterns of Cu/NCF sample.

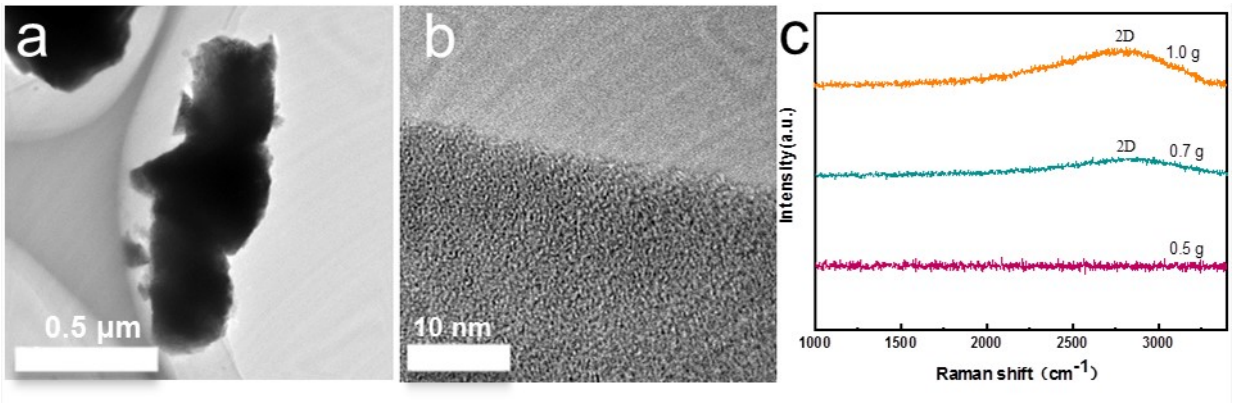

Fig. S7 (a) TEM image and (b) HR-TEM image of NC@NiCuCo-N/NCF, (c) Raman spectra of NC@NiCuCo-N/NCF used 0.5 g, 0.7 g and 1.0 g dicyandiamide, respectively.

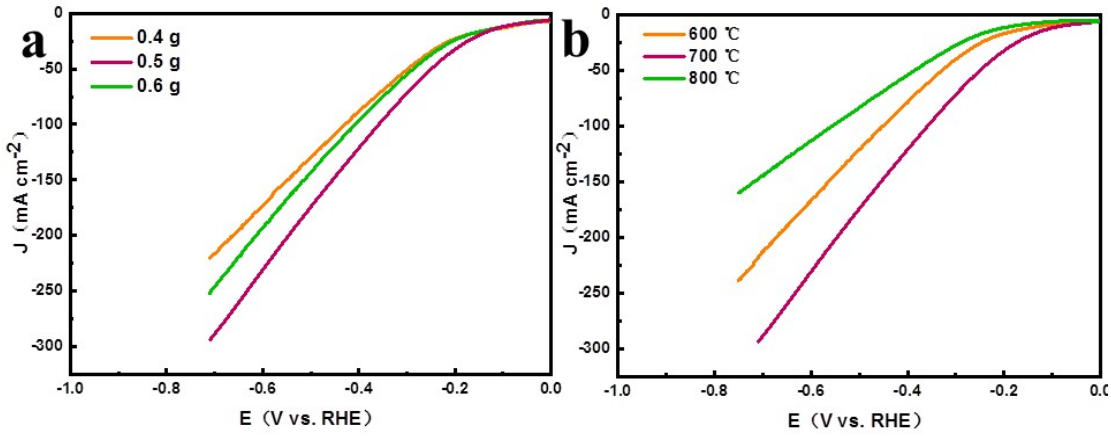

Fig. S8 (a) LSV curves of samples prepared with 0.4 g, 0.5 g, 0.6 g dicyandiamide and (b) LSV curves of samples prepared with (a, b) 600 ºC, (c, d) 700 ºC and (e, f) 800 ºC temperature in the nitriding process.

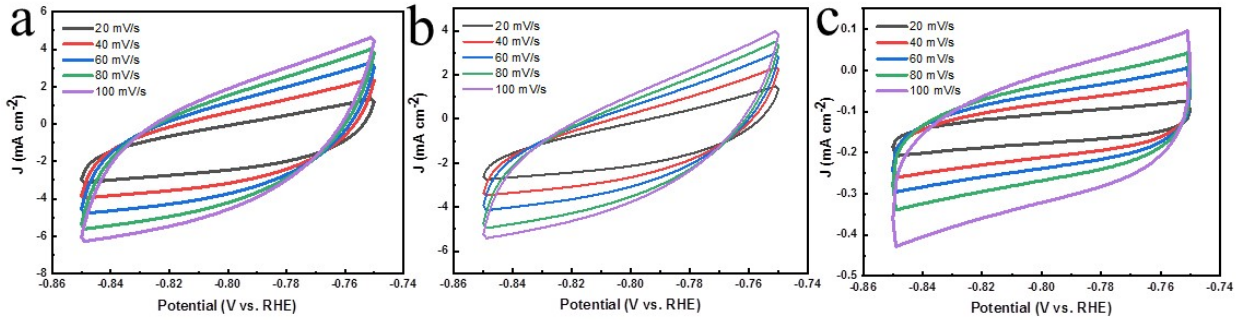

Fig. S9 CV curves in the non-faradaic capacitance current range at different scan rates for

(a) NiCoCu-N/NCF, (b) Cu/NCF, (c) NCF in 1M KOH electrolyte.

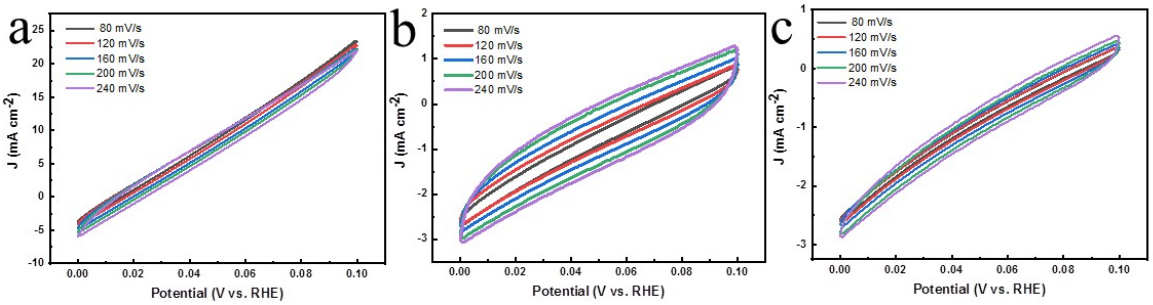

Fig. S10 CV curves in the non-faradaic capacitance current range at different scan rates for

(a) NiCoCu-N/NCF, (b) Cu/NCF, (c) NCF in 0.5 M H_2SO_4 electrolyte.

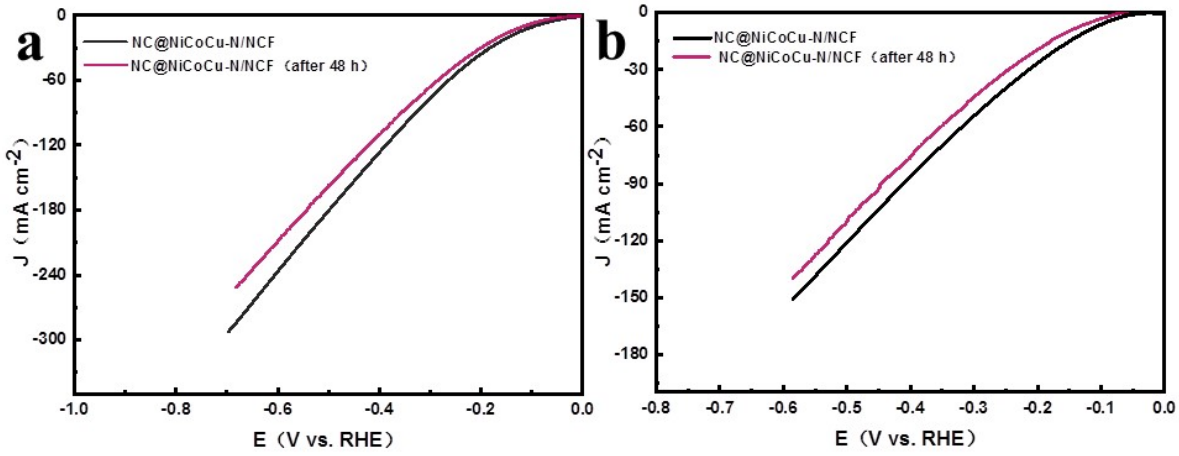

Fig. S11 LSV curves of NC@NiCuCo-N/NCF before and after stability test (a) in 1 M KOH and (b) in 0.5 M H_2SO_4.

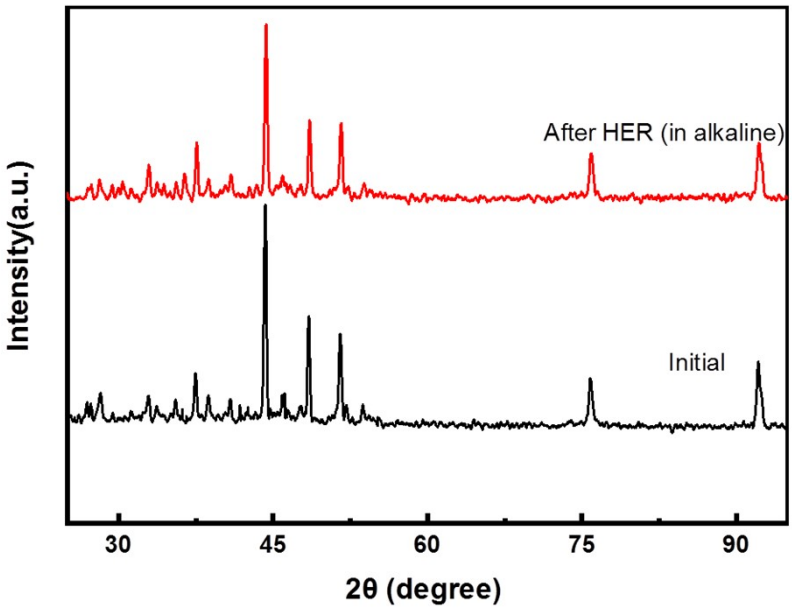

Fig. S12 (a) XRD comparison of NC@NiCuCo-N/NCF before and after stability test In 1 M KOH.

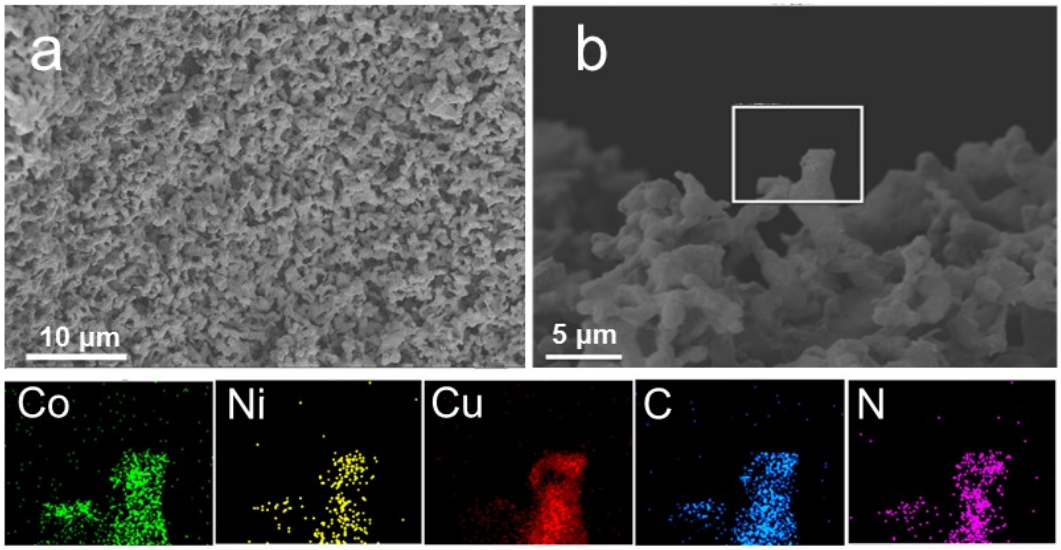

Fig. S13 (a) SEM image of NC@NiCuCo-N/NCF, (b) SEM image and EDX elemental mapping of Co, Ni, Cu, C, N after chronopotentiometric test in 1 M KOH.

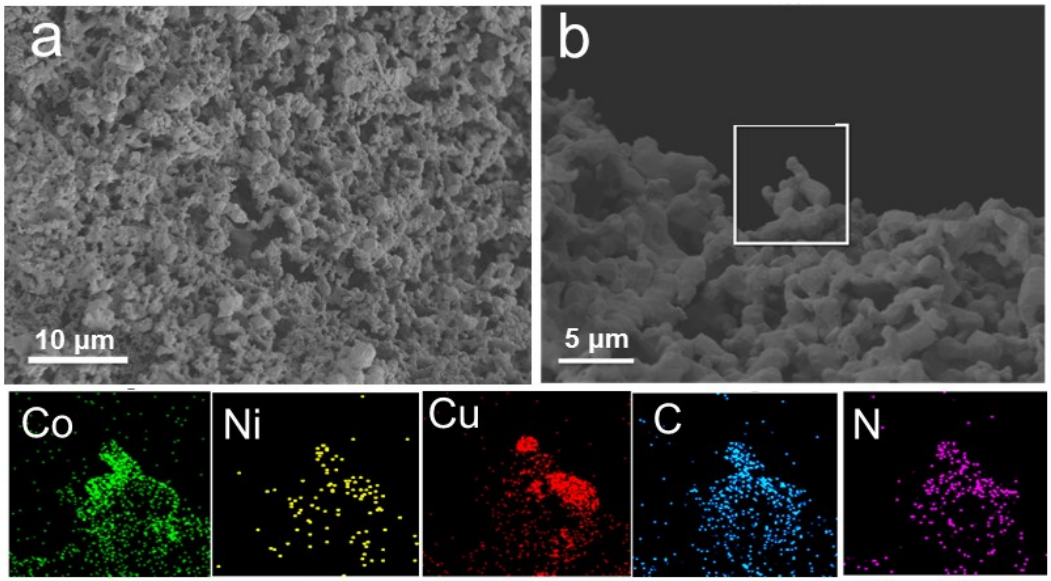

Fig. S14 (a) SEM image of NC@NiCuCo-N/NCF, (b) SEM image and EDX elemental mapping of Co, Ni, Cu, C, N after chronopotentiometric test in 0.5 M H_2SO_4.

Table S1 Comparison of HER performance of NC@NiCoCu-N/NCF with other advanced electrocatalysts in alkaline media.

Catalysts	**η_{10} (mV)**	**Tafel slope (mV dec^{-1})**	**References**
NC@NiCoCu-N/NCF	89	96	This work
Co/CoMoN/NF	61	68.9	[S1]
Cu/NiO/Cu_2O@NCF	79	60	[S2]
Co_3O_4-Co_4N	90	57.8	[S3]
Fe-Cu@CN3	91	117	[S4]
Ni/Mo_6Ni_6C@C	101	147	[S5]
$Ni(OH)_2$@Ni-N/Ni-C	102	43.9	[S6]
Co–N/CNT/C-850	120		[S7]
NC@CoN/Cu_3N/CF	134	99.2	[S8]
Co-NCNTFs//NF	141	/	[S9]
Co-NCNT/NF	157	88	[S10]
Ni–N–C/Ni@CNT-H	175	/	[S11]
Co@NMPC	193	64	[S12]
Co-Ni_3N	194	156	[S13]
$NiSe_2$/Ni-N-CNT	220	63	[S14]

Table S2 HER parameters of various as-prepared catalysts in 1 M KOH.

Catalyst	**η_{10} (mV)**	**Tafel slope (mV dec^{-1})**	**C_{dl} (mF cm^{-2})**	**Rct (Ω)**
NC@NiCuCo-N/NCF	89	96	31	2.25
NiCo-N/NCF	134	138	25	2.59
Cu/NCF	182	207	18	3.23
NCF	298	227	1.5	4.21

Table S3 HER parameters of various as-prepared catalysts in 0.5 M H_2SO_4.

Catalyst	**η_{10} (mV)**	**Tafel slope (mV dec^{-1})**	**C_{dl} (mF cm^{-2})**	**Rct (Ω)**
NC@NiCuCo-N/NCF	131	106	15	1.3
NiCo-N/NCF	182	169	7.3	1.8
Cu/NCF	221	234	3.8	4.2
NCF	365	269	1.3	5.7

Reference

[S1] H.B. Ma, Z.W. Chen, Z.L. Wang, C.V. Singh, Q. Jiang, Adv. sci., 2022, 9, 2105313.

[S2] J. Ren, Q. Wang, Q. Xiang, C.M. Yang, Y. Liang, J.H. Li, J.L. Liu, D. Qian, Chem. Eng. Sci., 2023, 280,119026.

[S3] B. Liu, J. Cheng, H.Q. Peng, D. Chen, X. Cui, D. Shen, K. Zhang, T. Jiao, M. Li, C.S. Lee, W. Zhang, J. Mater. Chem. A, 2019, 7, 775-782.

[S4] Q.F. He, H.Q. Liu, P.F. Tan, J.P. Xie, S.H. Si, J. Pan, J. Solid State Chem., 2021, 299, 122179.

[S5] Q.Q. Pan, C.Y. Xu, X. Li, J.F. Zhang, X.L. Hu, Y. Geng, Z.M. Su, Chem. Eng. J., 2021, 405, 126962.

[S6] K. Dastafkan, X.J. Shen, R.K. Hocking, Q. Meyer, C. Zhao, Nat. Commun., 2023, 14, 547.

[S7] Y.K. Fan, W.M. Duan, K. Xu, C.Z. Yan, C.C. Zheng, ACS Appl. Nano Mater. 2023, 6, 7920-7930.

[S8] J.L. Li, X.G. Kong, M.H. Jiang, X.D. Lei, Inorg. Chem. Front., 2018, 8, 2906-2913.

[S9] Q.Y. Yuan, Y.X. Yu, Y.J. Gong, X.F. Bi, ACS Appl. Mater. Interfaces, 2020, 12, 3592-3602.

[S10] R.J. Wang, L.J. Jiang, Q.L. Wang, G.F. Wei, X.F. Wang, Adv. Compos. Hybrid Ma., 2023, 6, 157.

[S11] L.L. Feng, C.L. Fu, D.M. Li, X. Ai, H.Y. Yin, Y.H. Li, X.Y. Li, L.Y. Cao, J.F.

Huang, Dalton Trans., 2023, 52, 9684-9693.

[S12] R. Jiang, Q. Li, X. Zheng, W.Z. Wang, W. Liu, S.B. Wang, Z.M. Xu, J. Peng, Int. J. Hydrogen Energ., 2022, 47, 27374-27382.

[S13] C.R. Zhu, A.L. Wang, W. Xiao, D.L. Chao, X. Zhang, N.H. Tiep, S. Chen, J.N. Kang, X. Wang, J. Ding, J. Wang, H. Zhang, H.J. Fan, Adv. Mater., 2018, 30, 1705516.

[S14] C.J. Wang, X. Zhang, Y.N. Zhu, K.L. Zhu, X.X. Luan, P. Yang, Electrochim. Acta, 2023, 454, 142386.